Available online at www.sciencedirect.com
SCIENCE DIRECT
ELSEVIER
International Journal of Refrigeration 28 (2005) 368–380
REVUE INTERNATIONALE DU FROID
INTERNATIONAL JOURNAL OF
refrigeration
www.elsevier.com/locate/ijrefrig

# CFD model of the airflow, heat and mass transfer in cool stores

H.B. Nahor[a], M.L. Hoang[a], P. Verboven[a,*,1], M. Baelmans[b], B.M. Nicolaï[a,2]

[a]*Flanders Center/Laboratory of Postharvest Technology, Department of Agro-Engineering and-Economics, Katholieke Universiteit Leuven, W. de Croylaan 42, B-3001 Leuven, Belgium*
[b]*Division of Applied Mechanics and Energy Conversion, Department of Mechanical Engineering, Katholieke Universiteit Leuven, Celestijnenlaan 300A, B-3001 Leuven, Belgium*

Received 21 April 2004; received in revised form 20 August 2004; accepted 25 August 2004
Available online 10 December 2004

**Abstract**

A transient three-dimensional CFD model was developed to calculate the velocity, temperature and moisture distribution in an existing empty and loaded cool store. The dynamic behaviour of the fan and cooler was modelled. The model accounted for turbulence by means of the standard $k$-$\varepsilon$ model with standard wall profiles. The model was validated by means of velocity, air and product temperature. An average accuracy of 22% on the velocity magnitudes inside the empty cold store was achieved and the predicted temperature distribution was more uniform than predicted. In the loaded cold store, an average accuracy of 20% on the velocity magnitudes was observed. The model was capable of predicting both the air and product temperature with reasonable accuracy.


*Keywords:* Cold store; Modelling; CFD; Heat transfer; Mass transfer; Speed; Air; Temperature; Humidity

# Modélisation par dynamique des fluides numérisée de l'écoulement de l'air et du transfert de chaleur et de masse dans les entrepôts frigorifiques

*Mots clés :* Entrepôt frigorifique ; Modélisation ; Dynamique des fluides ; Transfert de chaleur ; Transfert de masse ; Vitesse ; Air ; Température ; Humidité

## 1. Introduction

Agricultural products are subjected to heat and mass transfer during cooling and storage. Uniform cooling and storage of fresh product is difficult to attain in industrial cooling rooms, owing to the existence of an uneven distribution of the airflow [1,2], which affects the product quality, especially during long-term storage. Heat and mass transfer inside bins of products, particularly, becomes very important in maintaining good quality of stored products,

* Corresponding author. Tel.: +32 16 32 14 53; fax: +32 16 32 29 55.
*E-mail address:* pieter.verboven@agr.kuleuven.ac.be (P. Verboven).
† Member of IIR commission D1.
‡ President of IIR commission C2.

0140-7007/$35.00 
doi:10.1016/j.ijrefrig.2004.08.014

**Nomenclature**

| | |
|---|---|
| $A_c$ | heat transfer area of the cooler ($m^2$) |
| $A_{spec}$ | specific area ($m^2\ m^{-3}$) |
| $a$ | ratio of transversal pitch to pipe diameter (–) |
| $C$ | constant (–) |
| $c_p$ | heat capacity of product ($J\ kg^{-1}\ °C^{-1}$) |
| $D$ | diffusivity ($m^2\ s^{-1}$) |
| $E$ | Error (–) |
| $f_e$ | external force ($N\ m^{-3}$) |
| $f_{RES}$ | resistance of product in bins ($N\ m^{-3}$) |
| $g$ | gravity vector component ($m\ s^{-2}$) |
| $H$ | enthalpy ($J\ kg^{-1}$) |
| $h_c$ | heat transfer coefficient at cooler ($W\ m^{-2}\ °C^{-1}$) |
| $h_m$ | mass transfer coefficient ($m\ s^{-1}$) |
| $h_T$ | heat transfer coefficient ($W\ m^{-2}\ °C^{-1}$) |
| $h_{fg}$ | heat of evaporation/condensation ($J\ kg^{-1}$) |
| $k$ | geometry parameter (–) |
| $l$ | cooler length (m) |
| $m$ | moisture evaporation or condensation ($kg\ m^{-3}\ s^{-1}$) |
| $p$ | static pressure (Pa) |
| $p'$ | $p+\rho_0 g_j x_j$ (Pa) |
| $Q_V$ | heat removed (W) |
| $q$ | heat of respiration ($W\ m^{-3}$) |
| $r$ | volume fraction (–) |
| $T$ | temperature (°C) |
| $t$ | time (s) |
| $u$ | velocity component ($m\ s^{-1}$) |
| $\mathbf{u}$ | velocity vector ($m\ s^{-1}$) |
| $x$ | Cartesian coordinate (m) |
| $X$ | product moisture content ($kg_w\ m^{-3}$) |
| $Y$ | humidity ratio ($kg_w\ kg_{air}^{-1}$) |
| $z$ | number of tube rows in the cooler (–) |
| $\beta$ | thermal expansion coefficient ($°C^{-1}$) |
| $\lambda$ | thermal conductivity ($W\ m^{-1}\ °C^{-1}$) |
| $\mu$ | viscosity ($kg\ m^{-1}\ s^{-1}$) |
| $\rho$ | density ($kg\ m^{-3}$) |

*Sub and super-scripts*

| | |
|---|---|
| a | Air |
| *i,j* | index of Cartesian components |
| f | mixture, fan |
| *o* | reference value |
| p | Product |
| sat | Saturation |
| v | Vapor |
| w | Water |

and is mainly dependent on the interaction between the supply airflow and the bulk products. The variability of the cooling rate as well as the temperature of the product inside a cool store causes the product quality to deteriorate through either increased respiration at higher temperature or by chilling or freezing injury at lower temperature.

One of the main aims in designing storage enclosures is to ensure a uniform targeted temperature and humidity in the stored bulk products. The intricate transport mechanics and the complex geometry of a fully loaded cool store make it difficult to determine the optimal configuration and operation parameters of the store in an empirical way. A model-based approach can prove to be advantageous for design purposes with small added cost. With the increasing availability and power of computers together with efficient solution algorithms and processing facilities, the technique of Computational Fluid Dynamics (CFD) can be used to solve the governing fluid flow equations numerically.

A first step towards modelling cool stores loaded with agricultural products is representation of the heat and mass transfer inside bulk storages of agricultural products. Many models have been proposed with different levels of complexity such as uniform air-product temperature [3,4], thermal equilibrium [3–7] and internal temperature gradient [3] with mass transfer incorporated [8,9]. Airflow has been studied in ventilated enclosures for food preservation and processing [10–12]. To study the non-uniform temperature and moisture of a loaded cool store, only a few models have been proposed in the last 10 years. These models are limited to a two-dimensional one-phase model [13], or distributed dynamic model with only validation for temperature at two locations in the cool store [2]. Van Gerwen and Van Oort [14] used CFD to model 3D airflow and heat transfer in a refrigerated room for agricultural products and studied the effect of different configurations on the cooling effectiveness. However, no detailed information of the model, or the validation was reported. Mass transfer was not modelled in most of the cases. Hoang et al. [15] used CFD to model 3D airflow, heat and mass transfer in an industrial cool store for chicory roots. The latter was validated for the air temperature only (air velocity and product temperature were not validated).

The main objective of the present work was to model the transient three-dimensional airflow, heat and mass transfer in an empty and loaded cool store. The model was then validated using experimental data for velocity and temperature distributions of both air and product phases.

## 2. Method

### 2.1. Model formulation

A transient two-phase model of heat and mass transfer in a cool store was proposed. The governing equation

expressed in Cartesian coordinates $x_i$ ($i=1, 2, 3$) for the air phase read as follows:

$$\frac{\partial u_i}{\partial x_i} = 0 \tag{1}$$

$$\rho_a \frac{\partial}{\partial t} u_i + \rho_a \frac{\partial}{\partial x_i}(u_i u_j) = -\frac{\partial p'}{\partial x_j} + \frac{\partial}{\partial x_i} \mu_{TOT} \left( \frac{\partial u_j}{\partial x_i} + \frac{\partial u_i}{\partial x_j} \right) - \rho_0 g_i \beta (T - T_0) + f_{e,j} \tag{2}$$

$$\rho_a \frac{\partial}{\partial t} H + \rho_a \frac{\partial}{\partial x_i}(u_i H) = \frac{\partial}{\partial x_i} \left( \frac{\lambda_{TOT}}{c_{p,a}} \frac{\partial H}{\partial x_i} \right) \tag{3}$$

$$H = c_{p,f}(T - T_0) \tag{4}$$

$$c_{p,f} = Y c_{p,w} + (1 - Y) c_{p,a} \tag{5}$$

$$\rho_a \frac{\partial}{\partial t} Y + \rho_a \frac{\partial}{\partial x_i} u_i Y = \rho_a \frac{\partial}{\partial x_j} D \frac{\partial Y}{\partial x_i} \tag{6}$$

with $\mu_{TOT}$, the sum of laminar and turbulent viscosity (kg m$^{-1}$ s$^{-1}$) and $\lambda_{TOT}$, the thermal conductivity including a turbulence contribution (W m$^{-1}$ °C$^{-1}$).

Inside bins, the model was solved for the superficial air velocity. In the momentum equations, the external force $f_{e,j}$ contains the resistance of the products. The energy conservation equation incorporates (i) the convection heat transfer from the product phase to the air phase due to the temperature difference, (ii) the heat of respiration and (iii) the heat loss/generation due to evaporation/condensation of the water at the surface of the product. It was assumed that the moisture in the air was transferred by convection and diffusion, neglecting mass transfer inside the product. The system of equations for the air inside the bins then becomes:

$$\frac{\partial u_i}{\partial x_i} = 0 \tag{7}$$

$$\rho_a \frac{\partial}{\partial t} u_j + \rho_a \frac{\partial}{\partial x_i}(u_i u_j) = -\frac{\partial p'}{\partial x_j} + \frac{\partial}{\partial x_i} \mu \left( \frac{\partial u_j}{\partial x_i} + \frac{\partial u_i}{\partial x_j} \right) - \rho_0 g_i \beta (T - T_0) + f_{e,j} \tag{8}$$

$$\rho_a \frac{\partial}{\partial t} H + \rho_a \frac{\partial}{\partial x_i}(u_i H) = \frac{\partial}{\partial x_i} \left( \frac{\lambda}{c_{p,a}} \frac{\partial H}{\partial x_i} \right) + h_T A_{spec} (T_p - T_a) \tag{9}$$

$$H = c_{p,f}(T - T_0) \tag{10}$$

$$c_{p,f} = c_{p,a}(1 - Y) + c_{p,w} Y \tag{11}$$

$$\rho_a \frac{\partial (r_a Y)}{\partial t} + r_a \rho_a \frac{\partial}{\partial x_i} u_i Y - r_a \rho_a \frac{\partial}{\partial x_j} D \frac{\partial Y}{\partial x_i} = m \tag{12}$$

The evaporation ($m$) was calculated using a lumped model, neglecting the moisture diffusion inside product and assuming local equilibrium at the product surface (Eq. (13)).

$$m = -\frac{\partial X}{\partial t} = h_m A_{spec} (\rho_p^v - \rho_a^v) \tag{13}$$

where $h_m$ is the mass transfer coefficient calculated based on the Lewis correlation for heat and mass transfer (m s$^{-1}$); $\rho_a^v$ is the density of the water vapour in the air phase and $\rho_a^v$ is the water vapour density in equilibrium with the wet surface.

Inside the bins, the product temperature was calculated as follows:

$$\rho_p c_{p,p} \frac{\partial}{\partial t}(r_p T_p) = h_T A_{spec} (T_a - T_p) - h_{fg} m + r_p q_p \tag{14}$$

The fan and the tube heat exchanger in the cooler were not modelled in detail. Instead, they were modelled as a block covering the cooler dimension, with distributed resistance and body force applied to the cooler block. For the heat exchanger, the pressure loss per unit length over the whole cooler corresponds to the characteristics of the heat exchanger tube banks, which was taken from literature [16]:

$$f_{e,j}^{res} = \frac{\Delta p_{c,s}}{\Delta l} = -Ckz\rho \frac{1}{\Delta l} \frac{a_2}{2(a-1)^2} |\mathbf{u}| u_j \tag{15}$$

where $\Delta p_{c,s}$ is the pressure difference between the inlet and outlet of the cooler (Pa); $\Delta l$ the length of the cooler ($m$) where the resistance was applied (0.6 m); $z$ the number of tube rows (12); $k$ a geometry parameter (1.004); $a$ the ratio between the distance from one tube to its neighbour to the diameter of the tube (3.125) and $C$ a constant factor (0.68), which was calculated based on the working point of the cooling unit at a specific rotation speed, taken from the manufacturer's data. This equation was applied to the momentum equation in each direction.

The fan was modelled as a body force based on the head-capacity relationship of the fan:

$$f_{e,j}^{fan} = \frac{\Delta p_{f,t}}{\Delta l} = \frac{1}{\Delta l}(C_{1FAN} + C_{2FAN} u_j + C_{3FAN} u_j^2) \tag{16}$$

where the $\Delta p$ is the pressure difference between the outlet and inlet of the fan which is equal to the total fan pressure drop. Starting from the fan static pressure, which was taken from the fan curve supplied by the manufacturer, the pressure difference was calculated as the fan static pressure plus the term $\rho u_j^2/2$. The body force $f_{e,j}^{fan}$ was added in the momentum equation in the main direction of the local flow. Based on manufacturer's data, the parameters $C_{1FAN}$, $C_{2FAN}$, $C_{3FAN}$ were equal to $-59.6$, 165.1 and $-65.3$, respectively, and $u_i$ [m/s] is the superficial velocity in the flow direction. For the heat transfer, a lumped model was used to describe the heat exchange between the cooler unit

with the air. Convection exchanges were assumed to obey Newton's law of cooling. At the cooler, the heat $Q_{V,c}$ [W] which was removed from the air was calculated as:

$$Q_{V,c} = h_c A_c (T_c - T_a) \quad (17)$$

where $h_c$ is the heat transfer coefficient at the cooler (W $m^{-2}$ $°C^{-1}$); $A_c$ the total surface area of the cooler ($m^2$) and $T_c$ the measured cooler temperature (°C). The heat transfer coefficient and area of the cooler were taken from the manufacturer's manual.

### 2.2. Model parameters

The heat of respiration, the heat and mass transfer coefficients, the saturated partial vapour pressure and the latent heat of evaporation as a function of temperature were calculated with the equations and correlations proposed in Hoang et al. [7]. The product resistance to airflow was calculated using the Ergun equation. The equilibrium moisture content curve of the product ('Conference' pear, *pyrus communis* cv. Conference) was obtained from Nguyen et al. [17]. The specific surface area of the fruit was estimated from a correlation developed by Schotsmans [18] using available data for average characteristic dimensions and volume of the fruit. Moreover, thermal mass, heat transfer area and thermal properties of the different components of the cooler were obtained from manufacturer's manuals and literature data. Further model parameters are summarized in Table 1.

### 2.3. Geometry, boundary conditions and numerical method

The cool store used in this study was a pilot cool store at the Flanders Centre of Postharvest Technology (Leuven, Belgium) with the dimensions of 2.8 m width, 4.25 m depth and 3.6 m height (Fig. 1a). The cooling unit, situated in the top corner of the store opposite to the door side, consisted of two axial fans of 40 cm in diameter (positioned at the back of the cooling unit) which rotated at 900 revolutions per minute. The operating range of the fan was provided by the manufacturer. The nominal values of operation were quoted to be a flow rate of 2140 $m^3$/h, corresponding to a fan static pressure difference of 28 Pa, for each fan connected to the heat exchanger unit. Due to the symmetry of the store (empty), only half of the store was modelled. The geometrical model was bounded by the inner walls. The cooler unit was modelled as a block with two parts: cooler and heater. The geometry of the cooler unit was built up using 121 zones (blocks), each defining a sub-region of the flow domain. The blocks were coupled by sharing faces. The 3D geometry was covered by a body-fitted structured grid with 1,022,856 volumes (150×130×56 subdivisions, grid size 3.0×3.0×2.5 cm).

Table 1
Modelparameters

| Parameter | Value |
|---|---|
| Product bulk density ($\rho_b$) | 600 kg $m^{-3}$ |
| Product bulk porosity ($r_a$) | 0.4 |
| Density of pears ($\rho_p$) | 1000 kg $m^{-3}$ |
| Thermal conductivity of pears ($k_p$) | 0.52 W $m^{-1}$ $°C^{-1}$ |
| Specific surface area of pears ($A_{spec}$) | 82.0 $m^2$ $m^{-3}$ |
| Heat capacity of pears ($c_{p,p}$) | 3800 J $kg^{-1}$ $°C^{-1}$ |
| Cooler heat transfer area ($A_c$) | 44.6 $m^2$ |
| Heat transfer coefficient at the cooler ($h_c$) | 36 W $m^{-2}$ $°C^{-1}$ |
| Density of air ($\rho_a$) | 1.25 kg $m^{-3}$ |
| Heat capacity of air ($c_{p,a}$) | 1008 J $kg^{-1}$ $°C^{-1}$ |
| Viscosity of air ($\mu$) | $1.78\times10^{-5}$ Pa s |
| Diffusivity of water in air ($I$) | $2.9\times10^{-5}$ $m^2$ $s^{-1}$ |

For the loaded cool store, 8 bins of pears covered on top by a perforated plastic foil were stacked in two rows, each contained four bins on top of each other (Fig. 1b). For this configuration, half of the cool store was also modelled. The bin's walls with air gaps around were modelled explicitly as conducting walls.

The commercial code CFX4.4 was used for the numerical implementation of the model, using finite volume techniques. The diffusion-convection terms were discretised with the HYBRID scheme, accounting for the directional properties of the flow at high velocities, whilst avoiding large numerical diffusion when steep gradients are present [19]. The overall accuracy of the discretisation was first order. In order to save computational time, it was assumed that heat transfer did not influence the velocity field initially. The model was, therefore, solved for the velocity field to the steady state with the mass residuals reducing to less than $10^{-5}$ of the initial value and the residual for velocity reducing to less than $10^{-4}$ of the initial value. The model was then solved for heat transfer together with the momentum equations to account for the effect of buoyancy. The initial conditions were the generated velocity field, 20 °C uniform room temperature (empty store simulation) and 18.5 °C uniform room and product temperature (loaded store simulation). The discretisation in time was implicit and the time step was 300 s. A total of 12 iterations per time step were found satisfactory to achieve a low value of the residuals for the heat transfer equation. At the end of each time step, the enthalpy residual was typically reduced to less than $10^{-3}$ of the initial value. The simulation was carried out on a Pentium III PC, 1100 MHz with 1 Gb RAM memory, running the Windows2000 operating system. A CPU time of about 200 h was needed to simulate 70 h of cooling.

### 2.4. Validation method

#### 2.4.1. Velocity measurements

For quantitative local velocity measurements, there are several techniques available such as Laser Doppler Anemometry (LDA), particle image velocimetry (PIV), vane anemometry, pitot tubes and thermal anemometry. An omni-directional transducer (TSI 8475, St Paul, MN, USA) was found to be suitable for this application. The probe

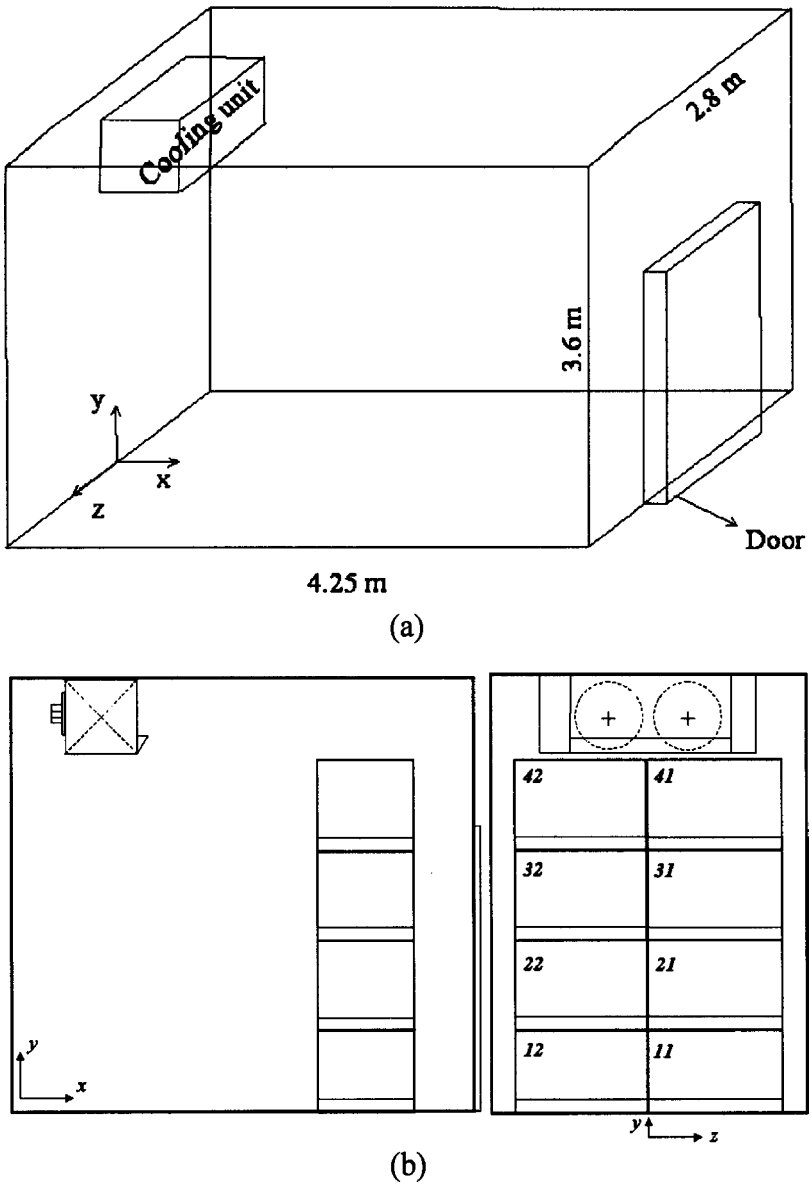


Fig. 1. (a) Empty cool store (b) Partially loaded cool store.

could be used to measure the time-averaged velocities, but did not give any information on flow turbulence due to the considerably long response time (5 s). The operating range (0.05–2.5 m/s) covered the range of velocities encountered in the cool room. In the factory calibration, the sensor was used with the main direction perpendicular to the sensor stem (accuracy $\pm 3\%$ of reading $\pm 1\%$ of full range). To check the omni-directional properties of the spherical sensor, additional calibration was done to account for the directional effect of the sensor stem to the sensor reading. The calibration was carried out with the calibration system StreamLine 90H10 (DANTEC, Skovlunde, Denmark) at the TME laboratory (Leuven, Belgium) for the velocity range from 0 to 1.5 m/s at two extreme cases of 90° (sensor stem perpendicular to the airflow) and 0° (sensor stem parallel with the airflow). In order to check the influence of the angle on the velocity reading the calibration was repeated for different angles (0–90°) at a velocity of 0.5 m/s. It was observed that when the measurement was done at an angle larger than 45°, the reading velocity was not influenced by the angle. When the angle was smaller than 45°, the sensor underestimated the velocity by about 20%. To average out this possible directional effect, the measurement value was first transformed by means of the two calibration curves at 0 and 90°. The average of the resulting values was taken as the measured velocity. The velocity transducer was then

connected to an Agilent Datalogger (Agilent, Palo Alto, CA, USA). The software Bench-link was used to interface with the data acquisition. 370 points in the empty cool room were scanned at three vertical planes, parallel to the cooler unit outlet and one horizontal plane, shown as solid lines in Fig. 2. The measurements were done with a mesh size of $\Delta x = \Delta y = \Delta z = 0.2$ m for $x$ larger than 1.85 m and $y$ limited to 2.9 m. The values between these grid points were linearly interpolated. In the loaded room, 26 points were scanned at the plane $x = 3.4$ m and $x = 2.89$ m (shown in dotted lines in Fig. 2). In the latter plane, measurements were carried out at the vertical gap close to the wall ($z = 1.3$ m) and horizontal gaps between the bins ($y = 0.1$; 0.8; 1.55 and 2.3 m). At each point (in both empty and loaded cases), the measurements were recorded at a time constant of 2 s and averaged over a 5 min period.

The error was calculated as the relative mean absolute difference between the measured and calculated velocity magnitude:

$$\bar{E}_{\mathrm{CFD}} = \frac{1}{n}\sum_{i=1}^{n}\frac{||u|^i_{\mathrm{CFD}} - |u|^i_{\mathrm{exp}}|}{|u|^i_{\mathrm{exp}}} \tag{18}$$

*2.4.2. Temperature measurements*

One hundred fifty and fifty five thermocouples were used in the empty and the loaded cool room, respectively, to measure both the air and product temperature. In the empty store, sensors were positioned in one half of the room at vertical intervals of 0.4 m in two $x$-planes ($x = 2.11$ m, and $x = 2.95$ m, $\Delta z = 0.3$ m) and one $z$-plane ($z = 0.7$ m, $\Delta x = 0.4$ m); at $z = -0.7$ m, symmetry was checked at selected positions. In the loaded cool room, the product temperatures in the middle of each bin were measured while the air temperatures were measured inside the bin at the front, the back and the side as well as in the free air. All thermocouples were calibrated in a temperature controlled water-bath (F-26, Haake, Germany) and ice water, for a temperature range from 0 to 30 °C. All sensors were connected to an Agilent Datalogger (Agilent, Palo Alto, CA, USA) and Bench-link software was used to interface with the data acquisition.

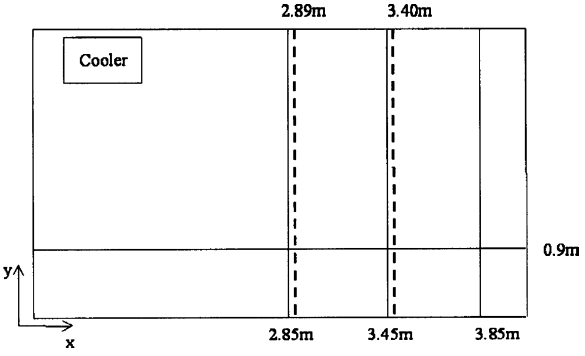


Fig. 2. Vertical and horizontal planes of velocity measurements in an empty (solid lines) and partially loaded (dotted lines) cool store.

*2.4.3. Weight loss measurements*

Pears were packed in very coarse-meshed bags with the initial weight of around 7.0 kg and located in the middle of every bin. Each bag was weighted before the cooling experiment and after 38 days of cooling and storage.

## 3. Results and discussion

### *3.1. Air velocity distribution*

*3.1.1. Empty cool store*

The model reached equilibrium at a flow rate of 2080 $m^3$/h, which was 2.8% less than the designed flow rate of 2140 $m^3$/h. This is due to the pressure drop in the cool store, which caused the total pressure drop to increase resulting in a lower mass flow of air. The general flow pattern is illustrated in Fig. 3, which shows the velocity in a vertical cross section of the cool store. After leaving the cooler, the air was accelerated, reached the ceiling and moved to the door. The air flowed downward and returned to the back of the room with a high velocity close to the floor. A low velocity region was observed in the middle of the store.

Calculated and measured average velocity magnitudes in three planes are given in Table 2. The average magnitudes of the calculated velocity were close to those of the measured ones. However, the relative error, calculated as shown in (Eq. 18), ranges from 19.5 to 23.5%. The largest error was found in the plane closest to the door ($x = 3.85$ m).

A qualitative comparison of the planes $y = 0.9$ m and $x = 2.85$ m is shown in Fig. 4. In general, good agreement was found for all the planes. The measurements in the $y$ plane (Fig. 4a) confirmed the validity of the symmetry assumption. However, the high velocity at the cooler side (left) was measured at the symmetry plane ($z = 0$), but was predicted at $z = 0.4$ m. A high velocity region was observed and predicted at the side wall (high $z$) and at the door end (high $x$). The velocity gradients in these two regions were larger in the measurements, while in the calculation these gradients were smoothed, especially at the door.

A comparison for a vertical plane ($x = 2.85$) is shown in Fig. 4b. It is clear that close to the side wall the air velocity was high, and gradually lower to the centre of the room. Right below the cooler unit, close to the wall, the air velocity was high. The model predicted this high velocity region but overestimated it. This may be due to excessive diffusion predicted by the model through the effect of the turbulent viscosity. At the floor, high velocities were found in the model, which is in agreement with the measurements.

*3.1.2. Loaded cool store*

In the prediction of the loaded store airflow, the cool air flowed out of the cooler and over the top of the bins, coming

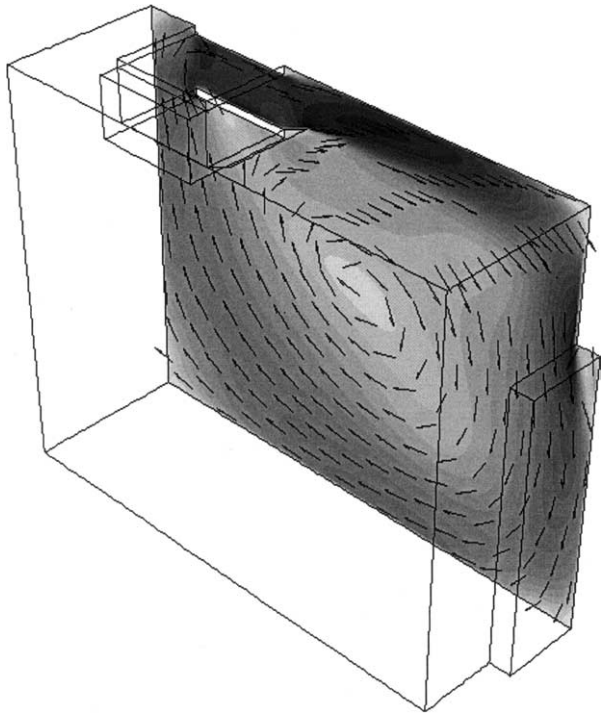

Fig. 3. Velocity magnitude (shaded contours) and flow direction (arrows) in a vertical section of the empty cool store through the cooler (fine grid, $k$-$\varepsilon$ turbulence model); velocity range from 0 to 2 m s$^{-1}$ corresponding to white and black, respectively).

back with high velocity close to the floor. High air velocity (exceeding 1 m s$^{-1}$) was observed at the side wall and close to the floor. There is some penetration of air through the horizontal gaps between bins and very little goes through the vertical air gaps around bins. Circulation of air occurred in the space between the bins and the cooler (Fig. 5). The quantitative comparison of the velocity magnitude is shown in Fig. 6. The average magnitudes of the calculated velocity were close to those of the measured ones. Over-estimation (up to 50%) was found close to the floor, and under-estimation was found at the upper bins. The overall absolute error of the CFD calculation was 20.4%.

In both the empty and loaded cases, the general airflow pattern is quite well predicted by the model. However, local discrepancies were found at the recirculation zones in both cases. The main reasons are believed to be the following.

- In general, the airflow in the room was not fully turbulent. According to Chen and Jiang [20], room airflow may be laminar unsteady, locally artificially induced turbulent, transitional or fully turbulent. Jones and Whittle [21] proved by experiments that the flow in the main body of ventilated rooms may be transitional. Barker et al [22] characterised room air motion as typically turbulent, although it is only weakly so. Barker et al. [23] showed that most room airflow is at least locally turbulent, but flows away from air supply systems and obstructions with edges tend to be subtly turbulent. Several authors reported that the standard version of the $k$-$\varepsilon$ model inadequately predicts the turbulence energy, $k$, in recirculation zones [19,24,25]. Through its effect on the viscosity, the local velocity distribution may be different from the actual distribution. This effect may be the main reason for the large discrepancy between measurements and model predictions in the centre of the room, where large recirculation exists in the case of an empty cool room, and near the top bin in the loaded store.
- Although the hybrid scheme for convection terms switches to second order accurate central differencing at low velocities, upwind differencing was used for high

Table 2
Distribution of the CFD calculation error on different planes

| Planes | $y=0.9$ m | $x=2.85$ m | $x=3.45$ m | $x=3.85$ m |
|---|---|---|---|---|
| Average measured velocity (m/s) | 0.50 | 0.46 | 0.45 | 0.63 |
| Average calculated velocity (m/s) | 0.53 | 0.45 | 0.48 | 0.65 |
| $\bar{E}_{\mathrm{CFD}}$ (%) | 20.5 | 19.5 | 23.2 | 23.5 |

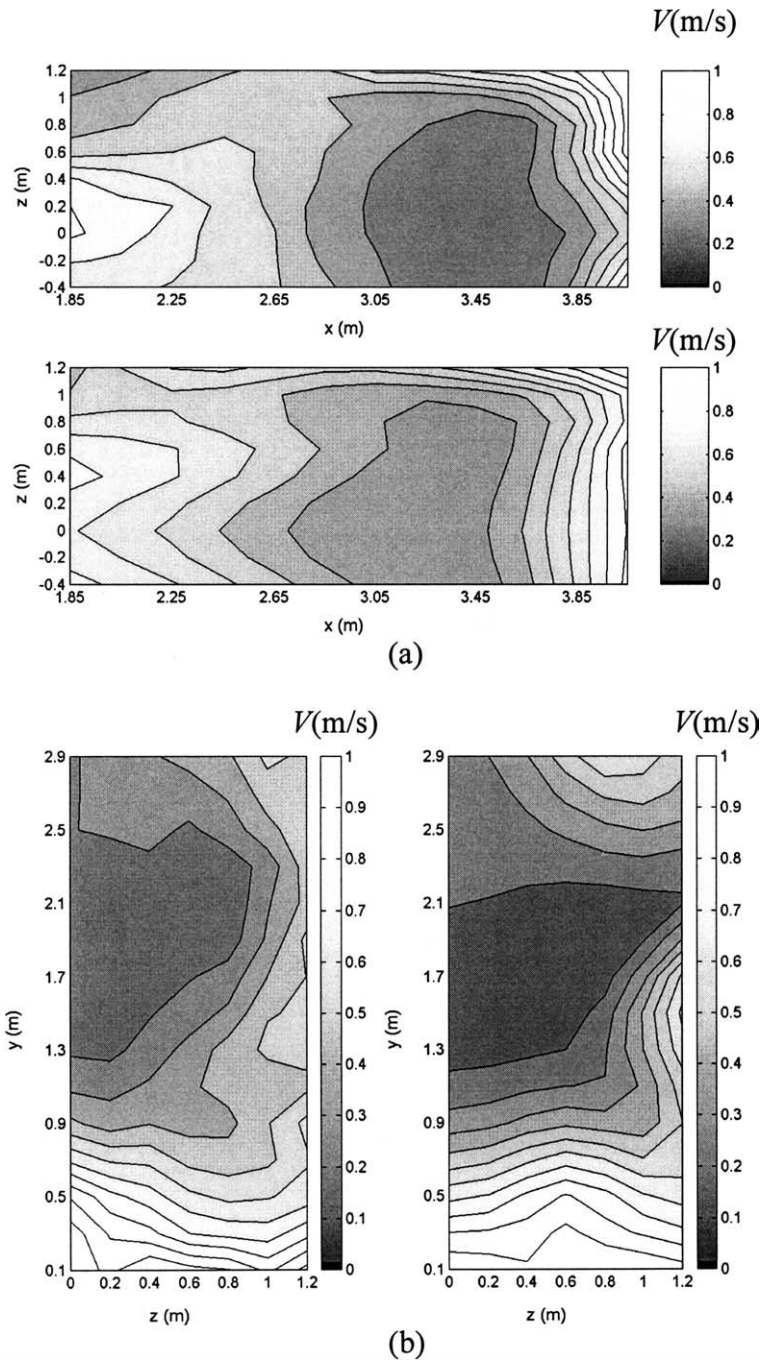


Fig. 4. Comparison of the CFD model predictions and the measurements of air velocity magnitude in an empty cool store at (a) $y=0.9$ m (measurement: upper; CFD: lower) and (b): $x=2.85$ m (measurement: left; CFD: right).

velocities and large grid sizes. With this type of interpolation the model solution was smeared out, rounding off peaks in the solution. This feature of the different schemes appeared clearly in the region where large velocity gradients existed: close to the wall (high $z$) and at the door (high $x$) in Fig. 4. Further grid refinement can be applied to improve the prediction in these regions. However, this was not possible due to limitation of computer resources. Besides, higher order schemes can be implemented but these schemes may sometimes produce physically unrealistic results and increase the computation time.

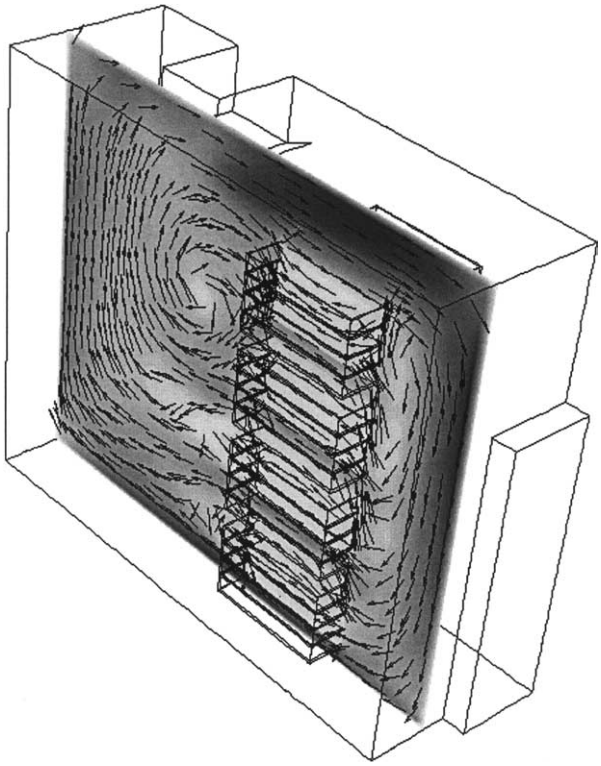

Fig. 5. Velocity magnitude (shaded contours) and flow direction (arrows) at plane $z=0.9$ m in a loaded cool store; velocity range from 0 to 2 m $s^{-1}$ corresponding to white and black, respectively.

- The experiment contributed to the error between the calculation and the measurement. As the direction of the flow in the cool store was not known, the measurement with the omni-directional velocity sensor has some difficulties in positioning the sensor in the right direction with the flow. Even though, calibration was performed with a transformation to obtain the averaged measured values, this is only an approximation of the velocity magnitude at each measured position.

### 3.2. Temperature distribution

#### 3.2.1. Empty cool store

Fig. 7 shows the measured time–temperature profiles at two different positions in the cool store during the cooling period representing the coldest and hottest points. The coldest point was located right in front of the cooler, while the hottest point was in the middle of the cool store. It is clear that the cooling rates at these two positions were considerably different as a result of the airflow. The increase near time 4000 s is due to the defrosting which was set every 4 h. The fluctuation of the temperature at steady state condition is attributed to the PID control actions for regulation of the room air temperature. It is shown that the model is capable of predicting the temperature during the cooling phase. The hot spot position was found to be the same in the measurement and simulation. However, while the measured temperature variation in the cool room was as large as 1.5° at steady state, the simulation showed a much more uniform temperature during cooling as well as at the steady state. This discrepancy can be explained by the circulating airflow pattern, as discussed earlier. The application of the turbulent model for an empty cool store, therefore, leads to a rather uniformly distributed temperature. At the end of the cooling period, the predicted air temperature followed the subcooling of the cooler temperature and gradually reached to the set point temperature.

#### 3.2.2. Loaded cool store

Fig. 8 shows the measured and predicted air temperature inside the bins at the bottom and the top of the stack, and at the front and at the back of each bin. It can be observed from the measurement that the defrosting cycle was set every 4 h. The air temperature at the front position reached the steady state condition after 12 h of cooling while it took about 40 h for the air at the back of the bin to reach steady state. This clearly affected the cooling rate of the product at these two positions. It can be observed from Fig. 8 that the model predicted the air temperature for the bins close to the floor quite well (Fig. 8a). The temperature difference between the measurement and prediction was in the range of the accuracy of the temperature measurement for the front

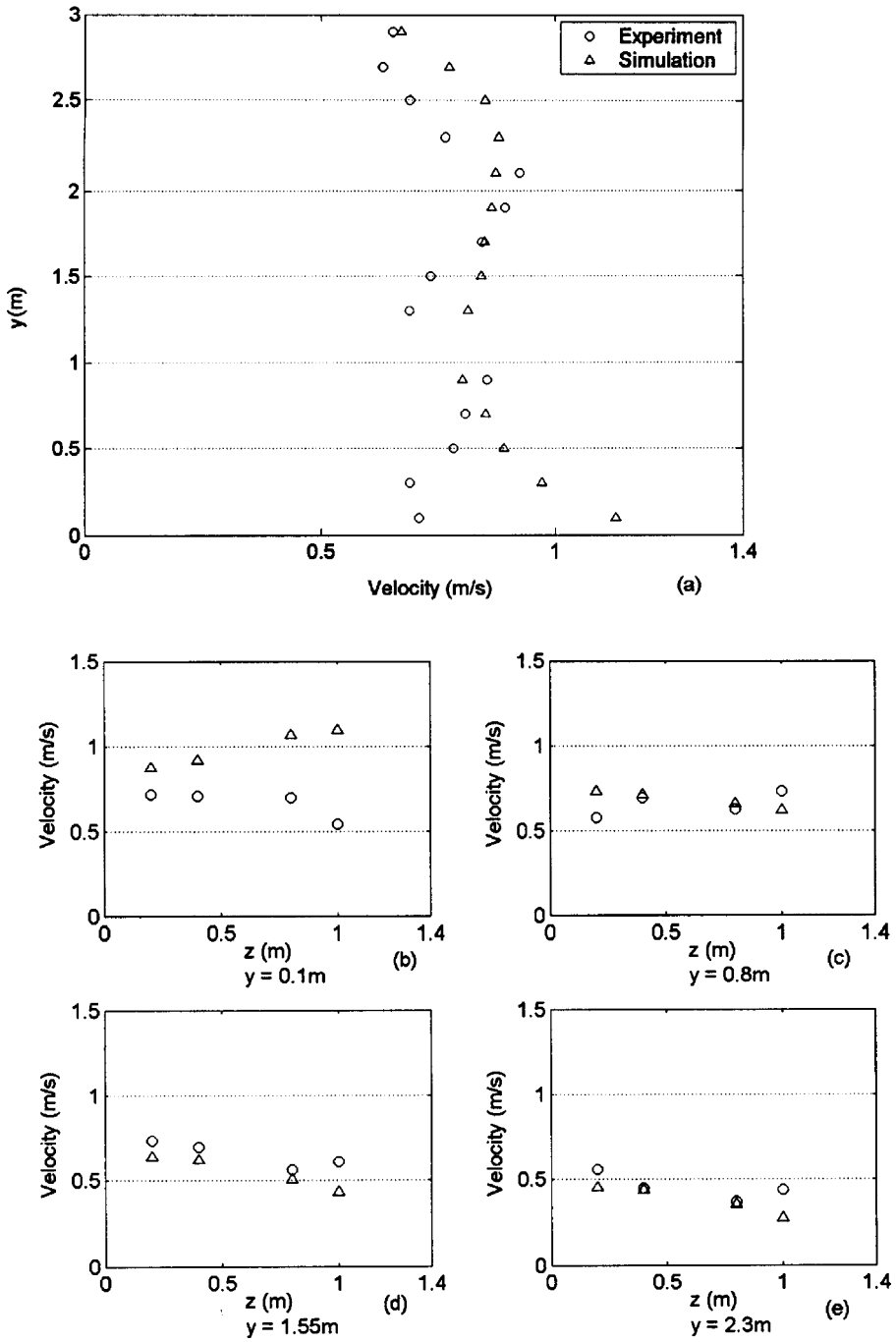


Fig. 6. Comparison of the CFD predictions and the measurements of air velocity magnitude at $x = 3.4$ m for (a) $z = 1.3$ m in the empty cool store and (b–e) horizontal lines $y = 0.1$, 0.8, 1.55 and 2.3 m in the loaded store, respectively.

positions. At the back of these bins, the model under predicted the air temperature. This under-prediction might be contributed by an over-estimation of the heat transfer coefficient for bulk product as well as an over-prediction of the air velocity in this region (Fig. 6b). Large discrepancy was found in the air temperature in the bin at the top (sensors 42F and 42B). The experimentally observed trends, however, were predicted well. The gradients from front (F) to back (B) were larger at the bottom than at the top and, at the center of the bin (position S, not shown), a faster drop in air temperature was observed at the bottom, in both the measurement and the model. This can be explained by a

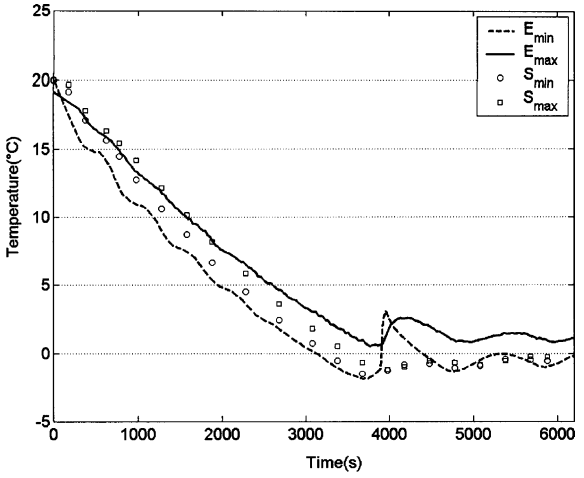


Fig. 7. Empty cool store temperature. E: experiment; S: simulation.

high air velocity at the lower bins, as seen in Fig. 5, and by comparing Fig. 6b (lower bin) and Fig. 6e (top bin): the average measured velocity at the bottom (0.65 $ms^{-1}$) is 40% higher than the top layer velocity (0.45 $ms^{-1}$), the modelled difference is larger. The predicted drop in air temperature at the top bin is clearly slower than observed, as seen in Fig. 8b. This difference should be attributed to the local airflow in the top bin: in the predictions the air penetrates the top bin from the top, resulting in a different pattern than for the other bins. Flow patterns inside the bins could not be verified, but as recirculating flows (see above) are not well predicted, this is believed to be the cause of the worse prediction at the top bin.

The measured and simulated product temperatures in the middle of the bins are plotted in Fig. 9. It can be observed that the initial temperature of the product inside bins varies from 16.8 to 18.5 °C. The variation in initial condition was not taken into account in the model and a uniform product temperature of 18.5 °C was applied. The product inside the lower bin (12 M) was cooled faster compared to the upper one (42 M), as a result of the observed higher velocity and lower air temperature. The model over-predicts the cooling rate of the product at all positions in the stack. The discrepancies can be explained by the following reasons:

- The model assumed no temperature gradient inside the product. Hence, an average temperature for the product phase was calculated which is evidently lower than the temperature at the centre of the product, where the measurement was done.
- The initial temperature differences inside bins were not taken into account. As the measurement points were only in the middle of the bins, their initial temperatures are not representative of the whole batch. The exact initial temperature distribution inside bins was, therefore, not known.
- The temperature prediction [7] is affected strongly by the heat transfer coefficient, calculated by an empirical formulation that may be inaccurate [26–28].

### 3.3. Weight loss

The weight loss of the product was measured after 38 days of cooling and storage only. It was observed that the average weight loss of all bins was $1.89 \pm 0.12\%$. Due to a long CPU time for each simulation (about 200 h for a simulation of 70 h of cooling), the weight loss of the product after 38 days was extrapolated based on the weight loss rate at the end of the cooling phase, when the product temperature attained the steady state. The simulated weight loss after 38 days of cooling varied from 1.9 to 2.2%, also

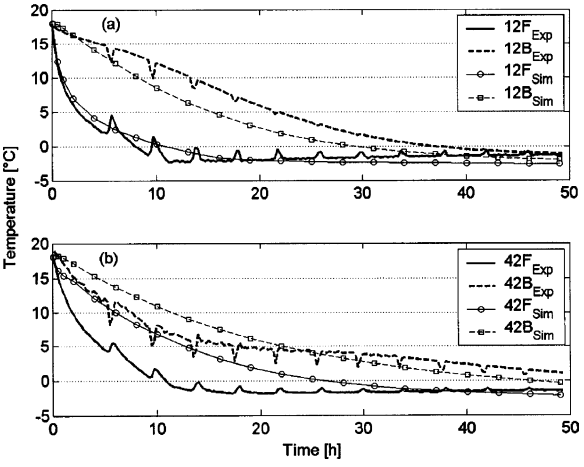


Fig. 8. Measured (Exp) and simulated (Sim) air temperature at the front (F) and back (B) positions inside bins (the numbers 12 and 42 refer to the position of the bins in the stack (see Fig. 1)): (a) bottom bin, (b) top bin.

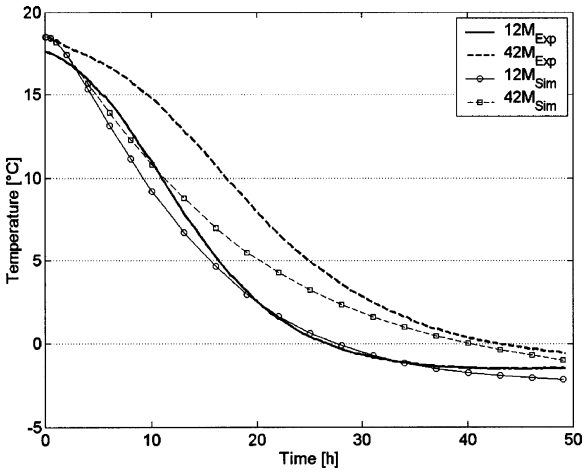


Fig. 9. Measured (Exp) and simulated (Sim) product temperature at the middle (M) of the bins (the numbers 12 (bottom bin) and 42 (top bin) refer to the position of the bins in the stack (see Fig. 1)).

indicating small differences. This was to be expected considering the small volume of the cool store considered and the small temperature variations observed at steady state.

## 4. Conclusions

A simplified model for 2-phase momentum, heat and mass transfer in an empty as well as loaded cool store with agricultural product was established to predict airflow around bins, air and product temperature as well as product weight loss. The model equations were solved and validated by means of experimental data from a pilot cool room. An error of about 20% for velocity magnitude prediction for both the empty and loaded cool store was achieved. The model was capable of predicting the cooling rate of the air as well as the product. Discrepancies in the temperature prediction are due to local under-prediction of the air velocity caused by the $k$-$\varepsilon$ turbulence model, the assumption of uniform initial temperature distribution inside bins and ignoring gradients inside the individual products. An error of 0.2% on the product weight loss after 38 days of cooling and storage was predicted. The model shows a rather good trend of cooling rate and weight loss rate of the product and can be used to study the effects of different parameters in the design and operation of industrial cool stores.

## Acknowledgements

The Flemish government and the Research Council of the K.U. Leuven are gratefully acknowledged for financial support. Author Pieter Verboven is a postdoctoral researcher with the Flemish Fund for Scientific Research (F.W.O. Vlaanderen).

## References

[1] P.S. Mirade, J.D. Daudin, Numerical simulation and validation of the air velocity field in a meat chiller, Int J Appl Sci Comput 5 (1) (1998) 11–24.
[2] H. Wang, S. Touber, Distributed dynamic modelling of a refrigerated room, Int J Refrigeration 13 (1990) 214–222.
[3] L.E. Lerew. Development of a temperature-weight loss model for bulk stored potatoes. PhD Thesis, Department of Agricultural Engineering, Michigan State University, Michigan, USA; 1978.
[4] R.G.M. van der Sman, Solving the vent hole design problem for seed potato packaging with the Lattice Boltzmann scheme, Int J Comput Fluid Dyn 11 (3–4) (1999) 237–248.
[5] K. Gottschalk, G.D. Christenbury, A model for predicting heat and mass transfer in filled pallet boxes. ASAE Paper No. 983157, 1998 July 12–16; Orlando (Florida), USA 1998.
[6] K.J. Beukema. Heat and mass transfer during cooling and storage of agricultural products as influenced by natural convection. PhD Thesis, Wageningen University, Wageningen, The Netherlands; 1980.
[7] M.L. Hoang, P. Verboven, M. Bealmans, B.M. Nicolaï, A continuum model for air flow, heat and mass transfer in bulk of chicory roots, Trans ASAE 46 (6) (2003) 1603–1611.
[8] Y. Xu, D. Burfoot, Simulating the bulk storage of foodstuffs, J Food Eng 39 (1999) 23–29.
[9] Y. Xu, D. Burfoot, Predicting condensation in bulks of food stuffs, J Food Eng 40 (1999) 121–127.
[10] P.S. Mirade, Prediction of the air velocity field in modern meat dryers using unsteady computational fluid dynamics (CFD) models, J Food Eng 60 (1) (2003) 41–48.
[11] J. Moureh, N. Menia, D. Flick, Numerical and experimental study of airflow in a typical refrigerated truck configuration loaded with pallets, Comput Electron Agric 34 (1–3) (2002) 25–42.
[12] M.L. Hoang, P. Verboven, J. De Baerdemaeker, B.M. Nicolaï, Analysis of airflow in a cool store by means of computational fluid dynamics, Int J Refrigeration 23 (2) (2000) 127–140.
[13] S.A. Tassou, W. Xiang, Modelling the environment within a wet air-cooled vegetable store, J Food Eng 38 (1998) 169–187.
[14] R.J.M. Van Gerwen, H. Van Oort, Optimisation of cold store design using fluid dynamics, Proceedings of the International Congress of Refrigeration 1990, Dresden, Germany, International Institute of Refrigeration, Paris, 1990. p. 473–478.
[15] M.L. Hoang, P. Verboven, M. Bealmans, B.M. Nicolaï, Analysis of the airflow, heat and mass transfer in chicory root cold stores by means of computational fluid dynamics, Proceedings of International Congress of Refrigeration, August 17–22, Washington DC, USA, International Institute of Refrigeration, Paris, 2003. [CD-ROM edition].
[16] A. Zukauskas, R. Ulinskas, Banks of plain and finned tubes in: G.F. Hewitt (Ed.), Handbook of heat exchanger design, Hemisphere, London, 1990.
[17] T.A. Nguyen, P. Verboven, N. Scheerlinck, E. Veraverbeke, B.M. Nicolai. An estimation procedure of effective diffusivity in pear tissue by means of numerical water diffusion model. Acta Horticalturae 599. In: Verlinden B, Nicolai B, De Baerdemaeker J, editors. Proceedings of the International Conference Postharvest Unlimited, 2003, 541–548.
[18] W. Schotsmans. Gas diffusion properties of pome fruit in relation to storage potential. PhD Thesis (557), Katholieke Universiteit Leuven, Leuven, Belguim; 2003.
[19] H.K. Veorsteeg, W. Malalasekera, An introduction to computational fluid dynamics—the finite volume method, Wiley, New York, 1995.
[20] L. Chen, Y. Li, Turbulent force flow in an air blast storage room, In: ROOMVENT'98, Proceedings of the 6th International Conference on Air Distribution in Rooms, June 14–17, Stockholm, Sweden, 1998 p. 451–458.
[21] P.J. Jones, G.E. Whittle, Computational fluid dynamics for building air flow prediction—current status and capabilities, Building Environ 27 (3) (1992) 321–328.
[22] A.J. Barker, P.T. Williams, R.M. Kelso, Numerical calculation of room air motion—Part 1: math, physics and CFD modelling, ASHRAE Trans 100 (1) (1994) 514–530.
[23] A.J. Barker, P.T. Williams, R.M. Kelso, Development of a robust finite element CFD procedure for predicting indoor room air motion, Building Environ 29 (1994) 261–273.
[24] B.B. Harral, C.R. Boon, Comparison of predicted and

measured airflow patterns in a mechanically ventilated livestock building without animals, J Agric Eng Res 66 (1997) 221–228.

[25] J. Borth, P. Suter, Influence of mesh refinement on the numerical prediction of turbulence airflow in rooms, In: ROOMVENT'94, Proceedings of the 4th International Conference on Air Distribution in Rooms, 15–17 June, Cracow, Poland (1994), pp. 137–148.

[26] F.P. Incropera, D.P. De Witt, Fundamentals of Heat and Mass Transfer, 3rd ed., Wiley, New York, 1990.

[27] R.B. Bird, W.E. Stewart, E.N. Lightfoot, Transport phenomena, 1st ed., Wiley, New York, 1960.

[28] R.B. Bird, W.E. Stewart, E.N. Lightfoot, Transport phenomena, 2nd ed., Wiley, New York, 2002.